3D INVERSE DESIGN BASED OPTIMIZATION OF MULTI-BLADE ROW AXIAL FANS USED FOR DISTRIBUTED PROPULSION

Mehrdad ZANGENEH [1], Peng WANG [2], Pedro GOMES [2]

[1] University College London, Department of Mechanical Engineering, Torrington Place, London WC1E -7JE, United Kingdom

[2] Advanced Design Technology Ltd, Dilke House, 1 Malet Street, London WC1E-7JN, United Kingdom

SUMMARY

In this paper a methodology is presented in which the geometry of a fan stage for aviation application is optimized to achieve maximum thrust for a given power input. The optimization method is based on coupling a 3D inverse design method together with ANSYS Workbench. Both chord distribution and 3D blade shape are modified by using 14 design parameters for both blade rows. The optimization process uses a multi-objective genetic algorithm on a surrogate model derived from the application of a Design of Experiments technique.

NOMENCLATURE

T	- Thrust [N]	ρ_0	- Free stream density [kg/m^3]
P	- Shaft power [W]	$\kappa_T = \frac{T}{\rho_0 N^2 D^4}$	- Thrust coefficient [-]
N	- Rotational speed [rev/s]	$\kappa_P = \frac{P}{\rho_0 N^3 D^5}$	- Power coefficient [-]
D	- Rotor shroud diameter [m]	$\varphi = \frac{\dot{m}}{\rho_0 N D^3}$	- Flow coefficient [-]
$\dot{m}$	- Mass flow rate [kg/s]		

INTRODUCTION

New stringent targets on emissions from aircraft such as EU's ACARE 2050 targets for NOx reduction by 90 % and CO_2 reduction by 75 % as compared to respective values in 2000 are encouraging the development new concepts for aircraft propulsion. One promising area of work is the development of so called distributed propulsion system, where a large number of fans are used appropriately at various locations on the fuselage to enhance propulsive efficiency, see [1] and [2]. One concept that is gaining ground is a ducted axial fan with rotor/stator configuration, see [3]. One key aspect of the design of these types of aviation fan is the requirement to maximize thrust for a given available power. This requires a different concept in design optimization of the fan stage.

Axial fans are conventionally designed by an iterative (direct) approach, which starts from an assumed blade shape whose performance is evaluated by CFD codes, see for example [4]. However, since the flow field is highly complex and 3D and there is no direct relationship between the blade geometry and flow field, the design process has to rely on the experience of designers. Generally speaking, experienced designers can achieve good designs by following closely what has worked in the past. However, such an approach can inadvertently result in a reduction of the design space as the designer tends to operate within their comfort zone. Hence using this approach will make it more difficult to achieve designs beyond previous experience (e.g higher pressure rise) or designs that meet contrasting multi-objective requirements on noise and efficiency.

An alternative method for aerodynamic design of fan blades is the inverse design approach, in which the blade geometry is computed for a specified distribution of blade loading. Since the blade loading is directly related to the pressure difference across the blade, the method allows the designer to directly control the 3D pressure field in the fan and hence have a more direct control over the viscous flow field. This approach removes the need for empiricism in the design process and allows designers to more directly explore a larger part of the design space.

A 3D inverse design code that has already been applied to many axial fan applications is TURBOdesign1 [5]. In this inverse design method the blade geometry is computed for a specified distribution of blade loading ($\partial r V_\theta$ / ∂m), which is the meridional derivative of the tangentially mean swirl velocity and is directly related to the blade bound circulation $2\pi\, r V_\theta$. In this method, in addition to the blade loading, the normal thickness distribution is specified therefore it is possible to ensure the structural integrity of the design. The method has already been applied to improve aerodynamic performance of axial fans and reduce broadband and tonal noise and improve efficiency, see [6], [7], [8] and [9].

In this paper the inverse design code TURBOdesign1 will be used together with ANSYS Workbench [10] to optimize the geometry of a ducted fan stage consisting of a rotor and stator to maximize thrust for a given power.

BASELINE FAN STAGE DESIGN

The baseline fan stage, consisting of an axial rotor and stator, was designed by using the 3D inverse design method subject to meeting the requirement for the thrust coefficient (Kt) of 1.90 and power coefficient (Kp) under 3.90 both at zero advance velocity and with flow coefficient (φ) of 1.13.

The baseline rotor and stator were first designed using TURBOdesign1. In this code, the rotational speed, the design flow rate, the number of blades, and the meridional geometry (i.e. axial chord) have to be specified. The initial axial chord distribution was provided by a meanline code, however it was manually modified as part of the design process.

The rotor was designed with constant hub and shroud radius (nevertheless the nose cone geometry is considered in the CFD analysis). A profile thickness distribution was used for it with maximum thickness of 7 % of the outer diameter (D) at the hub and 5.6 % at the shroud, maximum thickness is reached at mid-chord.

The volume flow rate was set based on the design flow coefficient and rotational speed. Once the basic design parameters and the meridional geometry are fixed three additional input specifications are required, the spanwise rV_θ, the blade loading ($\partial rV_\theta / \partial m$), and the stacking condition. The average value of spanwise rV_θ is directly related to the pressure rise at the design point, its streamwise variation affects the circulation distribution on the blade and is an important design parameter that directly influences boundary layer growth and secondary flows.

In the design of the rotor, initially a forced vortex spanwise rV_θ distribution was specified with higher value of rV_θ at the shroud and lower value at the hub with a linear variation. The meridional derivative of rV_θ is directly related to the pressure difference across the blade along each streamline and is therefore used to control the blade surface pressure distribution. The blade loading was controlled by specifying the distribution of $\partial rV_\theta/\partial m$ on the hub and shroud sections from which the 3D blade loading is constructed by interpolating along the spanwise direction. Both distributions were parameterized by means of a three-segment method (Figure 1), which employs a combination of two parabolic curves and an intermediate linear curve. The following four parameters are required to control each distribution:

- NC: intersection between the first parabolic segment and the linear segment.
- ND: intersection between the linear segment and the second parabolic segment.

- SLOPE: slope of the linear segment. This parameter controls the loading distribution type, a positive value leads to a fore-loaded distribution, a negative one leads to an aft-loaded distribution.

- DRVT: blade loading at the leading edge. This parameter controls the flow incidence and thus the inlet blade angle. If set to zero, a zero-incidence condition is imposed.
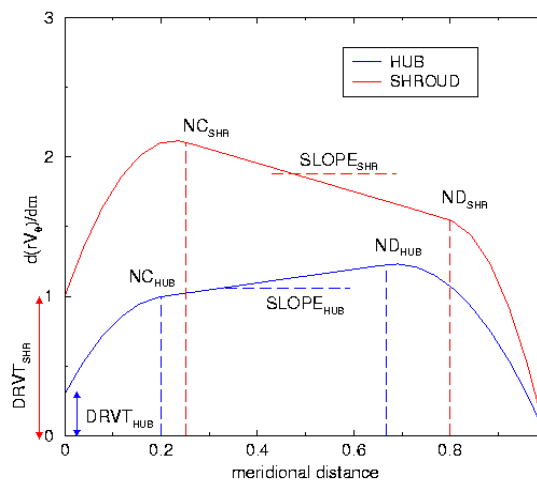

Figure 1: The method for specifying blade loading

The blade loading specified for the baseline design is shown in figures 2a and 2b. The baseline rotor was designed with zero incidence and a fore-loaded distribution that reduces friction losses.

Regarding the stacking condition, the wrap angle (i.e. θ−values of the camberline) distribution is specified along a single quasi-orthogonal line from the hub to the shroud. The stacking condition can affect the blade sweep and can have a significant effect on the 3D pressure field in the fan. For the baseline design, constant stacking with zero values of wrap angle was applied at mid-chord. A tip clearance of 0.43 % of D was assumed for the rotor. The rotor was designed with 14 blades.
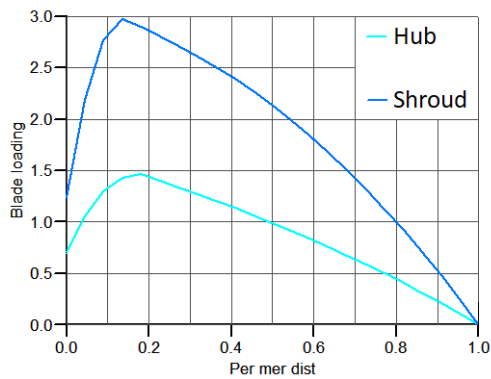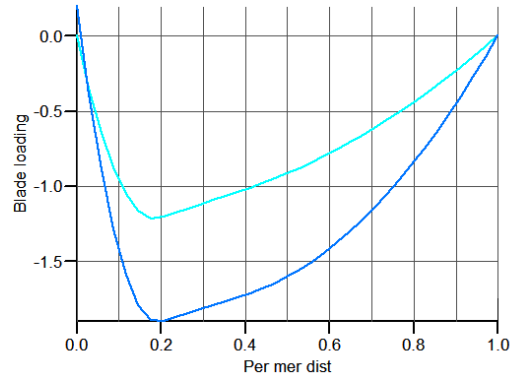
Figure 2a: Initial design rotor blade loading

Figure 2b: Initial design stator blade loading

The stator was designed with the same constant hub and shroud radius as that of the rotor. A profile thickness distribution was used for the stator with the hub peak thickness set at 60 % of axial chord and the shroud peak thickness at 25 % of axial chord. The same volume flow rate was used to design the stator and spanwise rV_θ at the leading edge of the stator was set to be the same value as at the exit of the rotor. The amount of exit rV_θ at the trailing edge was set to control the amount of diffusion and was also one of the parameters used to meet the thrust requirement for the fan stage. At the shroud it was possible to achieve axial outlet flow, at the hub however it was not possible to do so at reasonable levels of diffusion, a diffusion ratio (velocity magnitude at the leading edge divided by velocity magnitude at the trailing edge) of 1.4 was targeted.

The loading distribution used for the stator design is shown in Figure 2b. The number of stator blades was 17. The resulting initial stage geometry is shown in Figure 3.
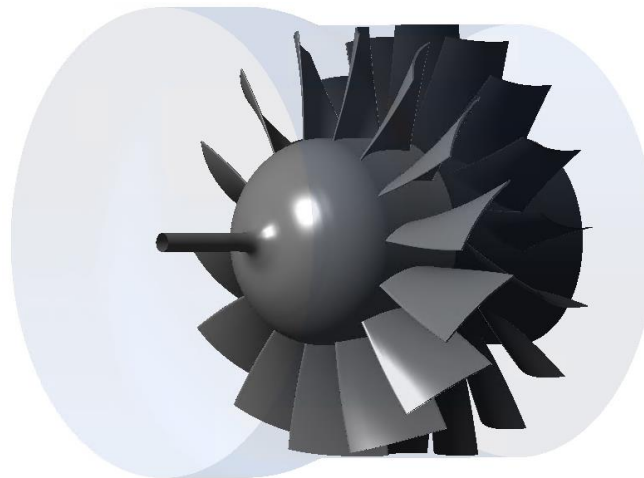

Figure 3: 3D geometry of the initial stage

ANALYSIS OF THE FLOW THROUGH THE BASELINE STAGE

The flow field through the baseline stage was analysed using ANSYS CFX 18.2 vertex centred, finite volume, coupled solver for the RANS equations in compressible flow.

The SST turbulence model was used with automatic blending between the viscous sub layer and log-law region. A surface average value of y+ over each wetted surface of 1 was targeted, the resulting total mesh size for the single passage model was approximately one million nodes, this resulted from keeping the maximum expansion rate below 1.3 and the maximum edge length ratio below 1000. The mesh was generated using the block structured mesh generator ANSYS TurboGrid, 20 layers are used to resolve the flow in the tip gap.

To verify the computational model a mesh sensitivity analysis was conducted, one coarser and two finer meshes were generated systematically, i.e. the controls defining the mesh size in the stream-, pitch- and span-wise directions were multiplied by a common factor. The thrust for the baseline stage was obtained for the four meshes, the results (normalized by the ones obtained with the 1M node mesh) are shown in Figure 4. The value of thrust varies 3 % from the coarsest to the finest mesh and does so monotonically, the reference mesh was therefore assumed to be sufficiently fine to resolve the features of the Reynolds averaged flow field.
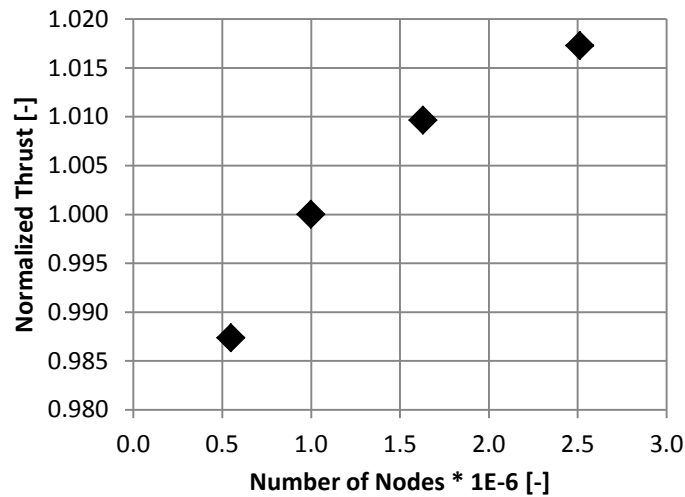

Figure 4: Thrust vs. node count

Total temperature and pressure are imposed at the inlet with the flow direction assumed to be normal. A mass flow boundary condition is used at the outlet.

The resulting computation of the thrust and torque confirmed that the stage meets the required value of K_t and K_p at the design flow coefficient. The flow field in the baseline stage was generally well behaved. The resulting surface streamlines on the stage are shown in Figures 5a and 5b.
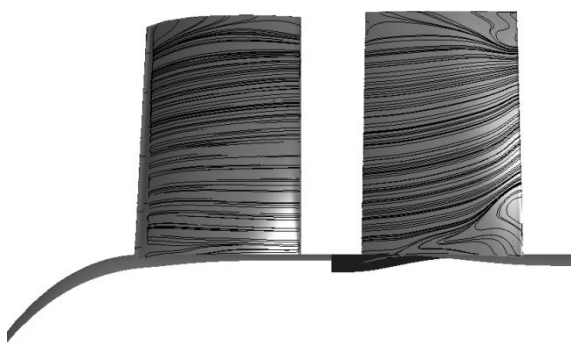

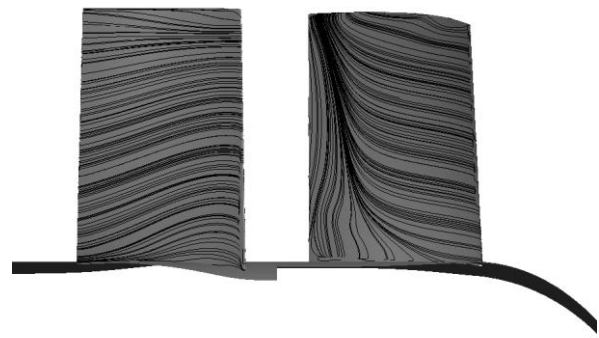*Figure 5a: Rotor pressure side*   *Figure 5b: Rotor suction side*

A region of separation, on the stator suction side near the hub, due to high diffusion can be observed. Near the shroud, the boundary layer thickness is large near the trailing edge, this occurs due to localized high incidence angle associated with the momentum deficit that arises from tip gap and end wall viscous effects, there is however no separation.

DESCRIPTION OF THE DESIGN STRATEGY

The aim of this study is to optimize the fan stage to maximise thrust for a given power coefficient.

For the multi-objective optimization of the fan stage TURBOdesign1 is integrated within ANSYS Workbench thus enabling automatic geometry transfer to ANSYS TurboGrid for mesh generation and subsequent CFD analysis in ANSYS CFX. This direct coupling of TURBOdesign1 inside ANSYS Workbench allows for a streamlined implementation of an inverse design based optimization strategy. The optimization capabilities within ANSYS Workbench are used to drive the optimization process.

The optimization methodology consists of two major steps, a sensitivity analysis to identify the most significant variables (out of a list of initial candidates), and their subsequent optimization by surrogate model based optimization.

The sensitivity information is obtained by fitting a linear response surface to a relatively small sampling of the design space, in this study 2n+1 samples were used (with n the number of candidate variables) to cover both the high and low end of each variable's range.

In the surrogate model based optimization step a multi objective genetic algorithm optimizer (such as NSGA II [11]) is asked to maximize thrust and minimize power based on mathematical models of these objectives. The model, typically a nonparametric regression or Kriging [10] (depending on goodness of fit), is built based on a finer sampling of the design space, in this study 8n samples are used (with n the number of optimization variables). The sampling of the design space is performed using Latin Hypercube sampling to generate a design matrix that is then populated by running the design (TURBOdesign1) and analysis (CFX) pipeline for each sample (i.e. stage design).

The Pareto front resulting from the optimization process allows choosing a candidate design considering the trade-off between power and thrust.

Blade Parameterization

The 3D inverse design code TURBOdesign1 is used to parametrically describe the blade geometry. Both the chord distribution of the rotor and stator and the blade loading parameters are varied.

The rotor chord is modified by controlling the axial coordinates of the leading edge at hub and shroud as shown in Figure 6 where the full range of variation is also illustrated. The coordinates are normalized by the meridional length of the respective curve (hub/shroud) and measured w.r.t. a reference location.
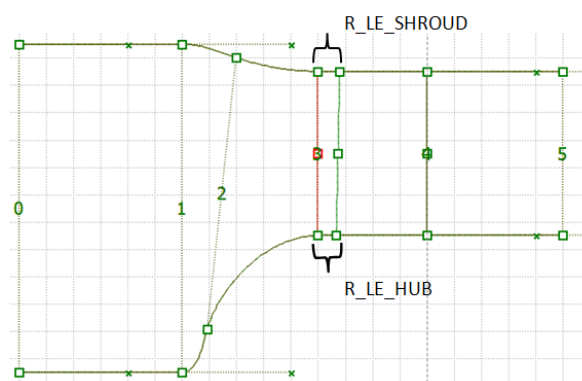

Figure 6: Parameters to control rotor chord and range of variation of the chord (red min, green max)

The chord distribution for the stator blade was modified by controlling the axial location of the leading edge at the shroud, the hub chord, and the axial location of the trailing edge at the shroud relative to the hub location, see Figure 7. The parameterization ensures a minimum spacing between rotor and stator blades, the parameters are normalized by initial hub chord.
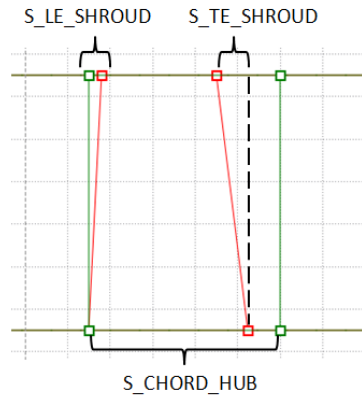
Figure 7: Parameters controlling stator chord and range of variation (red min solidity and green max)

The streamwise blade loading distribution on the rotor and stator was varied via the leading edge loading (DRVT_Hub and DRVT_Shroud) and the slope of the linear section (SLOPE_Hub and SLOPE_Shroud) parameters as shown in Figure 1, these variables are naturally normalized as they define the distribution of $\partial(rV_\theta/U\text{ref})/\partial\text{m}$ rather than $\partial rV_\theta/\partial\text{m}$ directly.

The design swirl distribution at rotor outlet / stator inlet was not changed, at stator outlet however, it was varied by controlling its value at the hub as this is the section where it is worth exploring the trade-off between trying to recover maximum static pressure or reducing flow separation. The variable is normalized by the product of tip radius and tip speed.

In total 14 design parameters were used for the sensitivity analysis, 5 control the chord distribution while the other 9 control the 3D blade loading.

OPTIMIZATION RESULTS

Sensitivity Analysis

Table 1 shows the ranges used for the 14 candidate variables, rotor variable names begin with "R_" and stator ones with "S_".

Table 1: Ranges used for the sensitivity analysis

Variable	Minimum	Maximum	Variable	Minimum	Maximum
R_LE_Hub	0.00	0.03	S_LE_Shroud	0.000	0.075
R_LE_Shroud	0.00	0.04	S_TE_Shroud	0.000	0.1875
R_SLOPE_Hub	-7	-2	S_SLOPE_Hub	2	8
R_DRVT_Hub	0.25	0.75	S_DRVT_Hub	-0.6	0.2
R_SLOPE_Shroud	-12	-4	S_SLOPE_Shroud	2	10
R_DRVT_Shroud	0.25	1.25	S_DRVT_Shroud	-0.6	0.2
S_CHORD_Hub	0.9375	1.125	S_RVT_Hub	0.1	0.3

After obtaining the thrust and power for the 2n+1 (29) designs generated to sample the design space defined in Table 1 linear response surfaces are fit to each output, the first order coefficients of the surfaces provide the sensitivities. As the parameters (input and output) vary in order of magnitude significantly, they are normalized to facilitate the interpretation of the results. Input parameters are translated and scaled to the range [0, 1] and output parameters are translated and scaled by their average value. With this normalization the value of a linear coefficient is interpreted as the mean variation of the output, relative to its average, when that input changes from minimum to maximum.

To use this information to reduce the number of variables used for optimization the ones with greater absolute value are chosen. Since there are two objectives their sensitivity values have to be

somehow combined into a single value used to sort the variables from most to least important. As the final objective is to maximize thrust for a given power one could consider a combined sensitivity for thrust minus power. However, it may also be desirable to have a significant variation in the Pareto front, for that the absolute values of the sensitivities for both outputs could be added. In this study both approaches are used and combined with equal weighing (after normalizing each so that the highest sensitivity is 1), the results are shown in Figure 8.
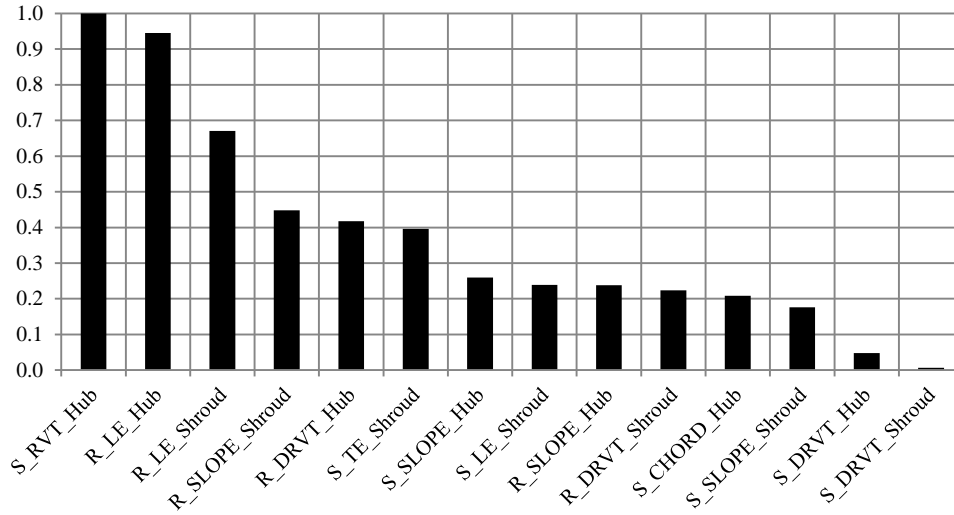

Figure 8: Results of the sensitivity analysis

The 7 most relevant variables will be used for optimization. This is obviously a compromise between the accuracy and the computational cost of the optimization but in the authors view and experience it is an acceptable one.

Optimization

If used only to reduce the number of variables, the cost of the sensitivity analysis would be substantial, however this need not be the case, the sensitivity information can be used to make adjustments to the values of the design parameters that will not be included in the optimization and to the ranges of the ones that will. In this study the ranges and values are adjusted by 25 % of the range depending on the sign of the sensitivities for the combined parameter thrust minus power, Tables 2 and 3 summarize this process.

The new design space defined in Table 2 was sampled with 8n design points (56) using Latin-Hypercube sampling. For 2 of these 56 designs the automated workflow failed to produce results, so 54 samples were used to build the response surfaces. Based on the results from cross-validation error analysis the nonparametric regression model was chosen over Kriging.

Table 2: Ranges used for optimization

Variable	Importance	Baseline	Min	Max	Kt-Kp	New Min	New Max
S_RVT_Hub	1	0.2	0.1	0.3	-2.263	0.05	0.25
R_LE_Hub	2	0.004	0.00	0.03	-0.542	-0.0075	0.0225
R_LE_Shroud	3	0.010	0.00	0.04	-0.187	-0.01	0.03
R_SLOPE_Shroud	4	-5	-12	-4	0.444	-10	-2
R_DRVT_Hub	5	0.70	0.25	0.75	0.753	0.375	0.875
S_TE_Shroud	6	0.0625	0.00	0.1875	-0.905	-0.047	0.141
S_SLOPE_Hub	7	2	2	8	-0.591	0.5	6.5

Table 3: Adjusted values before optimization

Variable	Importance	Baseline	Min	Max	Kt-Kp	New Value
S_LE_Shroud	8	0.025	0	0.075	0.529	0.044
R_SLOPE_Hub	9	-3.2	-7	-2	0.299	-1.95
R_DRVT_Shroud	10	1.2	0.25	1.25	0.187	1.45
S_CHORD_Hub	11	1	0.9375	1.125	0.282	1.047
S_SLOPE_Shroud	12	2	2	10	-0.403	0.0
S_DRVT_Hub	13	0.0	-0.6	0.2	-0.066	-0.2
S_DRVT_Shroud	14	0.2	-0.6	0.2	-0.009	0.0

The multi objective genetic algorithm optimizer was used obtain the trade-off (Pareto front) for thrust and power based on the aforementioned response surfaces, three candidate designs were chosen from the Pareto front and verified, Figure 9 shows the results of this process.
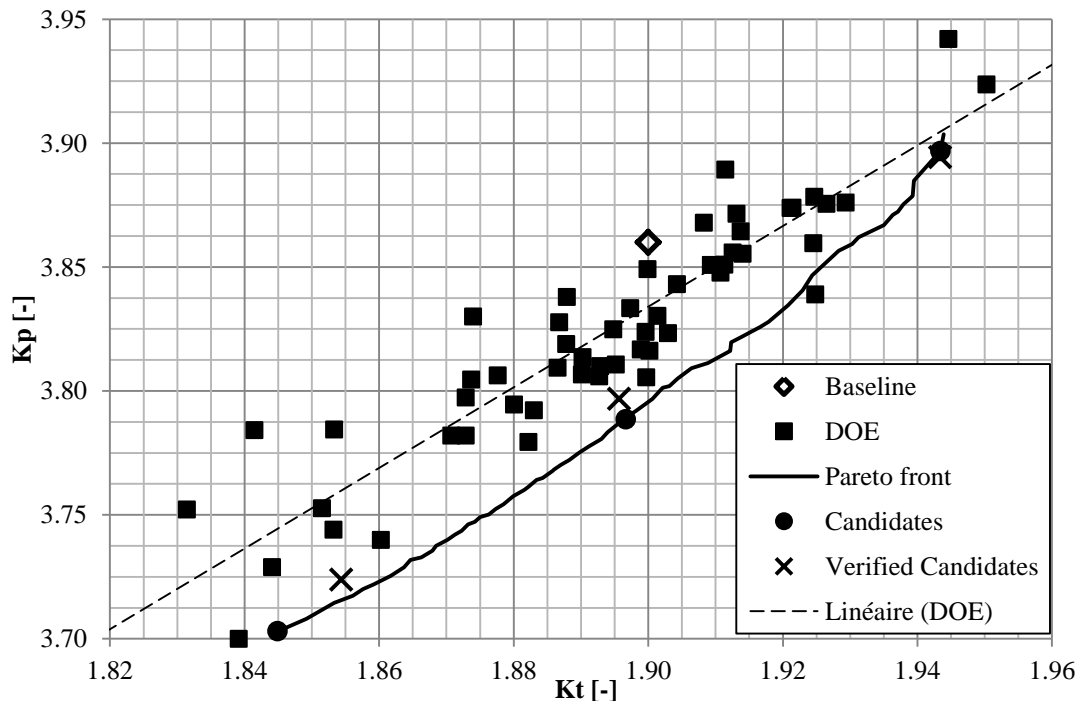

Figure 9: Pareto front from optimization

The response surface error is acceptable for the high thrust and the middle design but very high for the low power design. To achieve the lowest power the optimizer reduces the rotor chord to the minimum of the range. DOE techniques often do not sample the borders of the design space and so for the low power point, the error may be higher partly due to extrapolation, nonetheless the design is close to the Pareto front. In the Pareto sense the three candidates are better than the baseline.

Analysis

Table 4 shows the values of the design parameters for the low power and high thrust candidates.

The meridional geometries of rotor and stator are compared in Figure 10 and the blade loading distributions in figures 11a and 11b.

Table 4: Design parameters for low power and high thrust

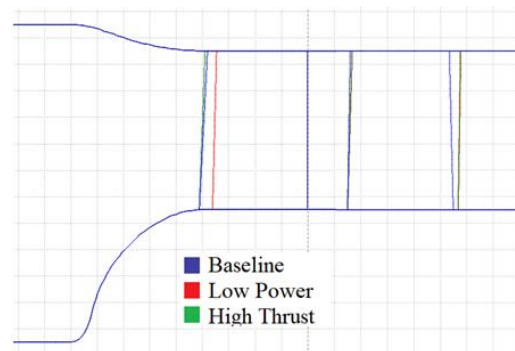| Variable	Baseline	Min	Max	Low Power	High Thrust
S_RVT_Hub	0.1	0.025	0.125	0.106	0.09
R_LE_Hub	0.004	-0.0075	0.0225	0.0174	-0.005
R_LE_Shroud	0.010	-0.01	0.03	0.027	0.005
R_SLOPE_Shroud	-5	-10	-2	-3.25	-7.7
R_DRVT_Hub	0.70	0.375	0.875	0.59	0.64
S_TE_Shroud	0.0625	-0.047	0.141	-0.018	-0.024
S_SLOPE_Hub	2	0.5	6.5	3.7	1.7

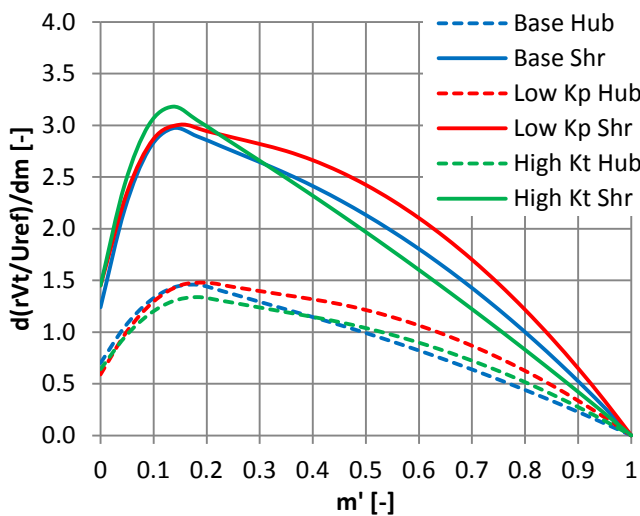*Figure 10: Stage meridional geometry comparison*

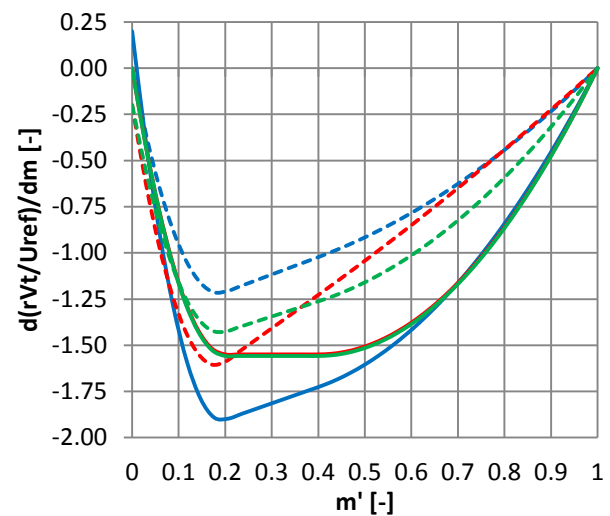*Figure 11a: Comparison of rotor blade loading*

Figure 11b: Comparison of stator blade loading

For low power the optimizer reduces the rotor chord almost to minimum, the loading at the shroud is adjusted in a way that maintains the value of peak loading, for this design the stator has to do less turning, possibly this allows the stator to be more fore-loaded without inducing significant separation.

For high thrust the optimizer increases the rotor shroud chord slightly and makes that section more fore-loaded. The stator is designed for lower outlet swirl at the hub, with this increase in stator loading it cannot be made as fore-loaded as the low power design.

Figures 12 and 13 show the flow field at 5 % and 95 % span for the low power and high thrust designs respectively.
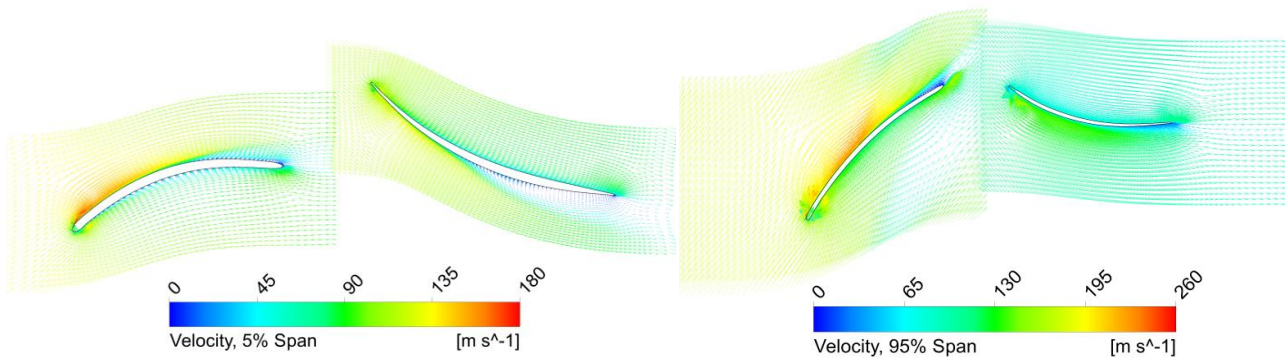
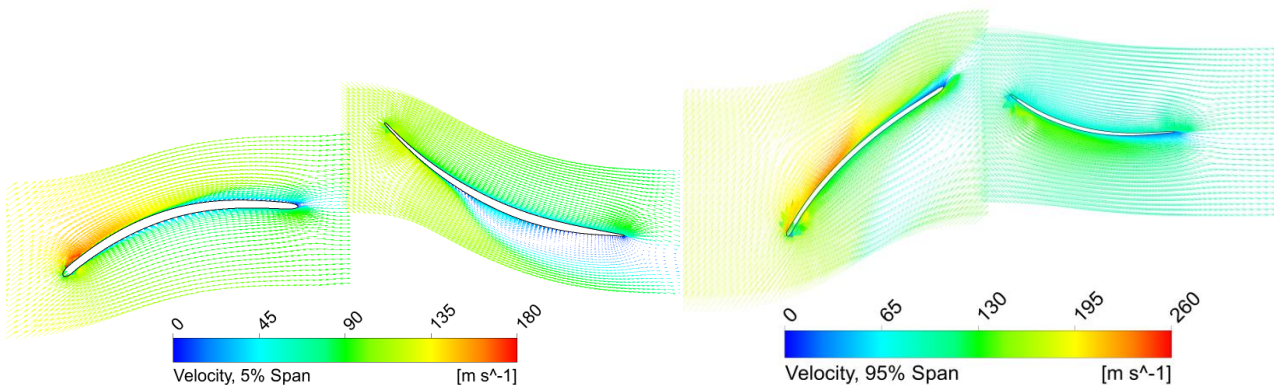*Figure 12: Hub and shroud flow field, low power design*

Figure 13: Hub and shroud flow field, high thrust design

For the high thrust design the stator hub separation starts earlier and is more severe than for the low power design, increasing thrust further without changing the parameterization would only be possible at the expense of significantly more power to overcome the mixing losses, this is also reflected in the shape of the Pareto front (high slope on the high thrust region).

Reducing power further with the current parameterization would also be difficult, because the rotor design rV_θ is the same, reducing its chord will at some point result in separation as the turning becomes excessive for the solidity. To cover a wider range of power/thrust the design rV_θ would have to be varied and the rotor chord should be parameterized as a function of it to avoid designs with insufficient solidity for their design rV_θ.

For the objective of this study, the parameterization was adequate as the target thrust coefficient is centred on the Pareto front. Compared to the baseline design it is possible to reduce K_p by 1.6 % for the same K_t or increase K_t by the same amount for the same K_p.

CONCLUSIONS

A methodology was presented for design of aviation fans with rotor/stator configuration in which 3D inverse design method is coupled with a multi- objective/multi-point automatic optimization strategy based on Design of Experiments, Surrogate model and Multi-Objective Genetic Algorithm. The methodology was applied to optimize the design of a generic baseline stage that needed a certain thrust for a given power. In total 14 design parameters, related to chord distribution, blade loading and spanwise rV_θ of both blade rows were used to parameterize the design. A two stage optimization strategy was performed. In the first stage a linear response surface was generated from a design matrix consisting of 29 geometries as generated by a Design of Experiment method

based on Optimal Latin Hypercube. The linear responses were then used to screen the 14 design parameters so that the most important 7 parameters are selected for more detailed optimization. The screening of the design parameters was on the basis of their effect on increasing thrust for a given power and taking account the sensitivity of the parameters on both thrust and power. Using the final selected 7 design parameters a design matrix consisting of 56 fan stages were generated and their performance evaluated to compute thrust and torque.   A surrogate model based on Kriging was then generated and a multi-objective genetic algorithm was then run on the surrogate model to establish the Pareto front between thrust and power. Three candidate points on the Pareto front were then selected and run in CFD. The resulting CFD computations of power and thrust for the 3 candidate points confirmed good correlation between surrogate model and actual CFD computations. The resulting designs for low power and high thrust have different characteristic in terms of blade loading and chord distribution on the rotor and stator.

The proposed inverse design based optimization strategy enabled the multi-objective optimization of the axial fan stage consisting of a rotor and stator for aviation propulsion application to be achieved with a total of 85 CFD computations and the resulting surrogate model showed high degree of accuracy versus CFD computations.

BIBLIOGRAPHY

[1]   H.J Steiner, A. Seitz, K. Wieczorek, K. Plotner, A. Isikveren, M. Hornung – *Multi-discplinary design and feasibility study of distributed propulsion system-* 28th International Congress of Aeronautical sciences – ICAS **2012**

[2]   H.D.Kim, J.L. Felder, M.T. Tong, M. Armstrong– *Revolutionary Aeropropulsion concept for sustainable aviation: Turboelectric distributed propulsion* – ISABE-2013-1719, **2013**

[3]   D.J. Eichenberg, C.A. Gallo, P.A. Solano, W.K. Thompson, D.R. Vrank – *Development of a 32 inch diameter levitated ducted fan conceptual design*, NASA-TM-2006-214481, **2006**

[4]   C. M Jang, M. Furukawa, M. Inoue – *Analysis of Vortical Flow Field in a Propeller Fan by LDV Measurements and LES Part I:Three-Dimensional Vortical Flow Structures*, Transactions of the ASME, Journal of Fluids Engineering, Vol 123, No.4, pp. 748-754, **2001**

[5]   TURBOdesign1 version 6.3 - Advanced Design Technology Ltd, **2016**

[6]   H. Okamoto, M. Zangeneh, H. Watanabe, A. Goto – *Design of a box fan rotor using 3-D inverse design method,* IMechE International Conference on Fans, 9-10 November **2004**, London.

[7]   K-Y Lee, Y-S Choi, Y-L Kim, J-H Yun – *Design of axial fan using inverse design method*, Journal of Mechanical Science and Technology, vol. 22 pp. 1883-1888, **2008**.

[8]   H. Okamoto, A. Goto, M. Furukawa – *Design Of A Propeller Fan Using 3-D Inverse Design Method And CFD For High Efficiency And Low Aerodynamic Noise*. ASME paper FEDSM 2009-78454, **2009**

[9]   M. Zangeneh and M. De Maillard – *Optimization of Fan noise by coupling 3D inverse design and automatic optimizer*, Fan 2012 conference, Senlis, France 18-20 April **2012**

[10]   B. Wilson, D. Cappelleri, T.W. Simpson, M. Frecker - *Efficient Pareto frontier exploration using surrogate approximations*, Optim. Engrg. 2 (**2001**) 31–50

[11]   K Deb, A Pratap, S Agarwal, T Meyarivan – *A fast and elitist multiobjective genetic algorithm: NSGA- II*, Evolutionary Computation, Vol 6, pp. 182-197, **2002**